The Journal of Experimental Biology 209, 433-443
Published by The Company of Biologists 2006
doi:10.1242/jeb.02017

Ontogeny of mantle musculature and implications for jet locomotion in oval squid *Sepioteuthis lessoniana*

Joseph T. Thompson* and William M. Kier

Department of Biology, CB#3280 Coker Hall, University of North Carolina, Chapel Hill, NC 27599-3280, USA

*Author for correspondence at present address: Department of Biology, Saint Joseph's University, 5600 City Avenue, Philadelphia, PA 19131, USA (e-mail: joe.thompson@sju.edu)

Accepted 28 November 2005

Summary

We examined the relationship between mantle muscle structure and mantle kinematics in an ontogenetic series (5–85 mm dorsal mantle length) of oval squid, *Sepioteuthis lessoniana*. Thick filament length increased during growth in the mantle muscle fibres that power jet locomotion (i.e. the circular muscles). The thick filament length of both the superficial mitochondria-rich (SMR; analogous to vertebrate red muscle fibres) and central mitochondria-poor (CMP; analogous to vertebrate white muscle fibres) circular muscles increased significantly during ontogeny. Thick filaments in the SMR circular muscle fibres of newly hatched squid (*N*=5) ranged from 0.7 to 1.4 μm and averaged 1.0 μm, while the thick filaments of the SMR fibres of the largest squids (*N*=4) studied ranged from 1.2 to 3.4 μm and averaged 1.9 μm. The ontogeny of thick filament length in the CMP circular muscle fibres showed a similar trend. The range for hatchling CMP circular muscles was 0.7–1.4 μm, with an average of 1.0 μm, whereas the range and average for the largest squids studied were 0.9–2.2 μm and 1.5 μm, respectively. Within an individual hatchling, we noted no significant differences between the thick filament lengths of the SMR and CMP fibres. Within an individual juvenile, the thick filaments of the SMR fibres were ~25% longer than the CMP fibres. The change in thick filament length may alter the contractile properties of the circular muscles and may also result in a decrease in the rate of mantle contraction during jetting. In escape-jet locomotion, the maximum rate of mantle contraction was highest in newly hatched squid and declined during ontogeny. The maximum rate of mantle contraction varied from 7–13 muscle lengths per second in newly hatched squid (*N*=14) and from 3–5 muscle lengths per second in the largest squids (*N*=35) studied.

Key words: cephalopod, obliquely striated muscle, thick filament, ontogeny, jet locomotion.

Introduction

Post-embryonic change in musculoskeletal systems is common in animals (e.g. Goldspink, 1983; Kelly, 1983; Werner, 1987; Kier, 1996). Such ontogenetic modifications may affect the ecology of the animal (Calder, 1984; Werner, 1987; Stearns, 1992) and provide insight into the evolution of form and function, yet they are often neglected in studies of physiology and comparative biomechanics.

For example, at hatching, cephalopod molluscs are broadly similar in form to adults (Boletzky, 1974; Sweeney et al., 1992), yet these tiny hatchlings may grow several orders of magnitude in size, shift from the neuston or plankton to the benthos or nekton (Marliave, 1980; Hanlon et al., 1985) and may use different mechanisms to capture prey (O'Dor et al., 1985; Chen et al., 1996; Kier, 1996) and for locomotion (Villanueva et al., 1995; Thompson and Kier, 2001a,b, 2002). In many cases, these life cycle changes are correlated with physiological and morphological changes that may have important effects on the locomotor performance or ecology of the animal.

Squid mantle muscle

In the mantle (Fig. 1) of loliginid squids, the family that has been studied most intensively, skeletal support for the mantle contractions that are used for locomotion by jet propulsion and for ventilation of the mantle cavity is provided by a complex arrangement of muscle and collagenous connective tissue fibres (Young, 1938; Ward and Wainwright, 1972; Bone et al., 1981). The mantle includes two predominant muscle orientations: circumferential muscle fibres (known as circular muscles), which constitute the bulk of the mantle wall, and radial muscle fibres that extend from the inner to the outer surface of the mantle wall as partitions between the blocks of circular muscle fibres (Fig. 1; Marceau, 1905; Williams, 1909; Young, 1938). Each circular muscle fibre is uninucleate, 1–2.5 mm in length, up to 10 μm in diameter and electrically

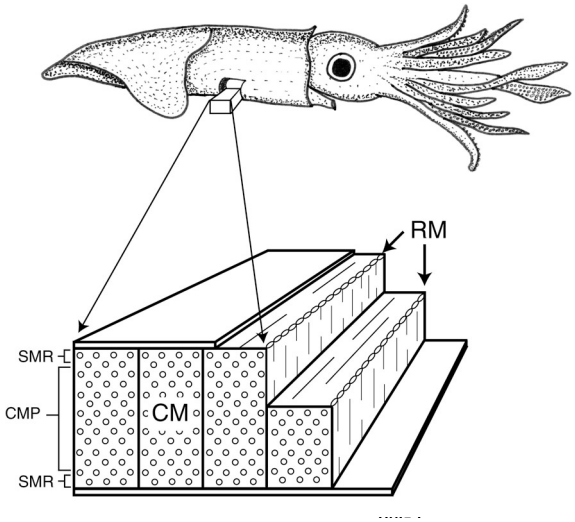

Fig. 1. Schematic of the mantle musculature. CM, circular muscles; CMP, central mitochondria-poor circular muscles; RM, radial muscles; SMR, superficial mitochondria-rich circular muscles. Modified from Kier and Thompson (2003).

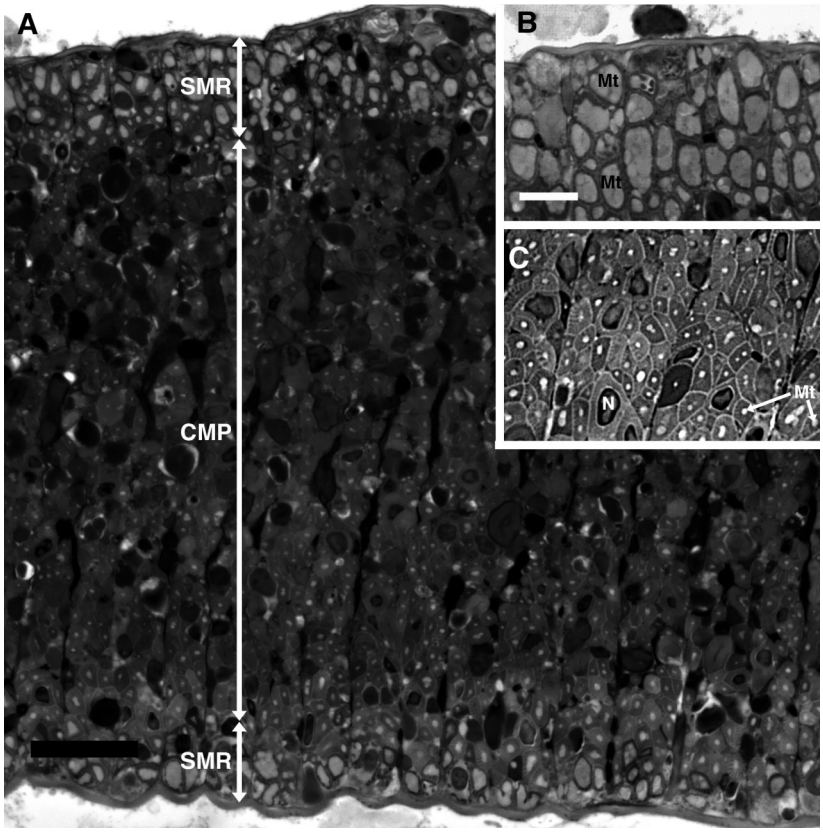

Fig. 2. Sagittal view of the mantle of a newly hatched *Sepioteuthis lessoniana* that shows (A) the relative proportions of superficial mitochondria-rich (SMR) and central mitochondria-poor (CMP) circular muscle fibres. Scale bar, 50 μm. A magnified view of SMR fibres is visible in B. Note the large size of the mitochondrial core (Mt) relative to the CMP cells in C. Note also that the cross-sectional area of myofilaments is not substantially different between the SMR (B) and CMP cells (C). The scale in B and C is the same. Scale bar in B, 10 μm. Bright-field microscopy of 1 μm glycol methacrylate sections stained with 1% Toluidine Blue. Mt, mitochondrion; N, nucleus.

coupled to adjacent circular muscle fibres, presumably by gap junctions (Marceau, 1905; Young, 1938; Hanson and Lowy, 1957; Millman, 1967; Moon and Hulbert, 1975; Bone et al., 1995; Milligan et al., 1997). The radial muscle fibres are also uninucleate and may be up to 5 μm in diameter (Bone et al., 1981; Mommsen et al., 1981). In both radial and circular muscles, the myofilament array surrounds a core of mitochondria and the single nucleus (Marceau, 1905; Hanson and Lowy, 1957). In addition, both are obliquely striated (Marceau, 1905; Hanson and Lowy, 1957; Kawaguti and Ikemoto, 1957). At resting length in *Loligo* spp., the striation angle (angle of alignment of z elements relative to the long axis of the cell) is 6–12°; when contracted, the angle increases to 14–18° (Hanson and Lowy, 1957).

The circular muscle fibres of loliginid squids are differentiated into three zones: an outer zone adjacent to the external surface of the mantle, a central zone and an inner zone adjacent to the inner surface of the mantle (Fig. 1). The circular muscle fibres of the inner and outer zones, known as superficial mitochondria-rich (SMR; Fig. 2) fibres (Preuss et al., 1997), contain large cores occupied by many mitochondria, show high succinic dehydrogenase (SDH) activity and have a large ratio of oxidative to glycolytic enzymes (Bone et al., 1981; Mommsen et al., 1981). By contrast, the circular muscle fibres of the central zone, termed central mitochondria-poor (CMP; Fig. 3) fibres (Preuss et al., 1997), have few mitochondria, low SDH activity and a low ratio of oxidative to glycolytic enzymes (Bone et al., 1981; Mommsen et al., 1981). The blood supply to the zones parallels these differences and includes a denser capillary plexus in the inner and outer zones compared with the central zone (Bone et al., 1981).

Ontogeny of muscle mechanics

In vertebrates and many arthropods, modulation of the contractile and mechanical properties of the musculoskeletal system often involves differential expression of muscle or connective tissue protein isoforms. The contractile properties of the flight muscles of dragonflies, for example, change during ontogeny; the change is correlated tightly with the expression of different isoforms of troponin T (Marden et al., 1998; Fitzhugh and Marden, 1997). Similarly, some skeletal muscles in newborn mammals exhibit initially low shortening velocity, which then increases rapidly during growth as the muscles express more fast-twitch myosin ATPase (e.g. Buller et al., 1960; Gauthier et al., 1978). The dimensions of the myofilaments and sarcomeres of vertebrate skeletal muscles, however, do not change with growth (Goldspink, 1968, 1983).

In cephalopods, the factors that affect the ontogeny of musculoskeletal mechanics have not been studied as intensively as in the vertebrates and arthropods. The existing work, however, suggests that modulation of the contractile properties of the muscles of squids and cuttlefishes may occur primarily through changes in the arrangement and the dimensions of the myofilaments, with little change in biochemistry (Kier, 1985; Kier and Schachat, 1992; Kier and Curtin, 2002).

In the oval squid, *Sepioteuthis lessoniana* (Family Loliginidae), the kinematics and mechanics of escape-jet locomotion change significantly during growth from the hatchling to juvenile stage (Thompson and Kier, 2001a, 2002). This provides an opportunity to test the hypothesis that changes in mantle muscle structure occur in synchrony with ontogenetic changes in the kinematics of the mantle during jet locomotion. To test the hypothesis, we used S-VHS video and high-speed digital video records of tethered and freely jetting hatchling and juvenile *S. lessoniana* to measure mantle contraction velocity during escape-jet locomotion. In addition, we used transmission electron microscopy to compare the lengths of the thick myofilaments in the circular muscles of the hatchlings and juveniles.

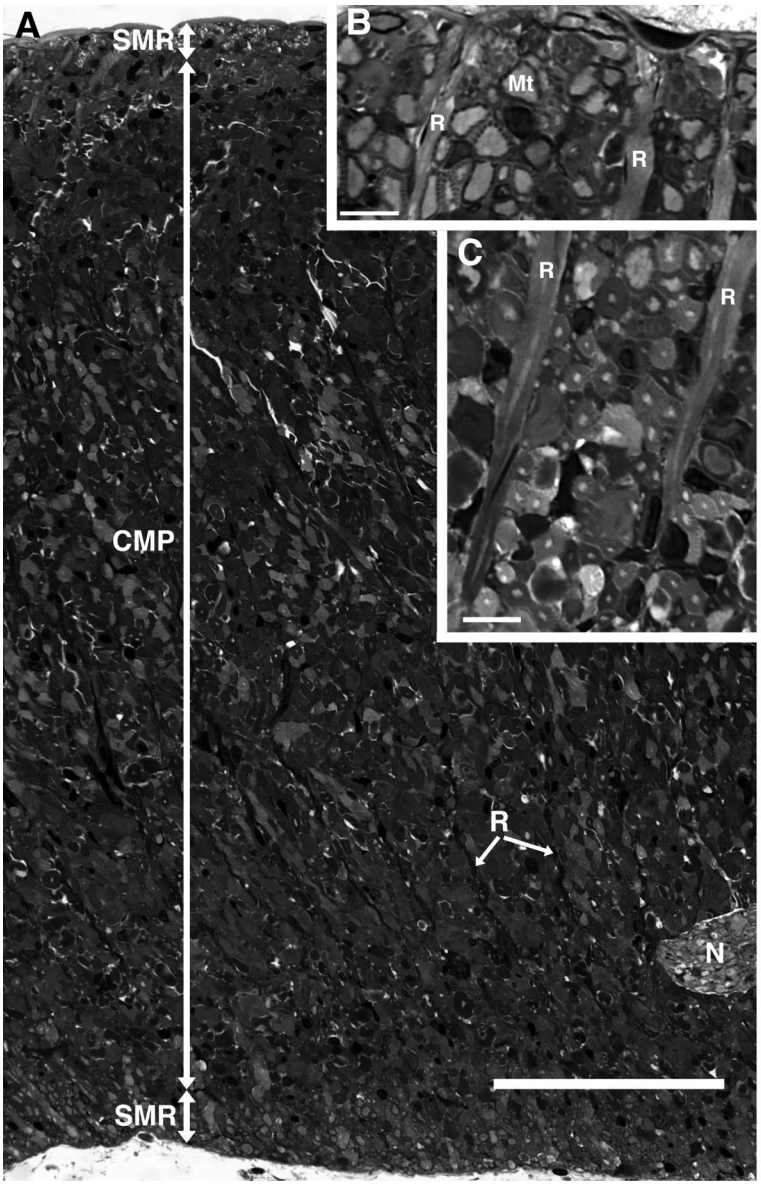

Fig. 3. Sagittal view of the mantle of a juvenile *Sepioteuthis lessoniana* that shows (A) the relative proportions of superficial mitochondria-rich (SMR) and central mitochondria-poor (CMP) circular muscle fibres. A nerve (N) and radial muscle fibres (R) are also visible in the micrograph. Compare A with Fig. 2A and note that juveniles have a much larger proportion of CMP to SMR circular muscle fibres. B and C show magnified views of the SMR and CMP cells, respectively. Scale bars in B and C are 10 μm. Bright-field microscopy of 1 μm glycol methacrylate sections stained with 1% Toluidine Blue.

Materials and methods

Animals

An ontogenetic series of *Sepioteuthis lessoniana* Lesson 1830 was supplied by the National Resource Center for Cephalopods (NRCC) at the University of Texas Medical Branch, Galveston, TX, USA. Wild embryos collected between 1999 and 2004 from several near-shore locations (Gulf of Thailand; Okinawa Island, Japan; Izo, Japan) were reared as described in Lee et al. (1994).

Commencing at hatching and at regular intervals thereafter, live squid were sent *via* overnight express shipping from the NRCC to the University of North Carolina at Chapel Hill, NC, USA or to St Joseph's University, Philadelphia, PA, USA. The squid ranged in size from 5 to 85 mm dorsal mantle length (DML) and in age from newly hatched to nine weeks post-hatching. Segawa (1987) separated *S. lessoniana* into seven size classes based on morphological and ecological characteristics: Hatchling, Juvenile 1, Juvenile 2, Young 1, Young 2, Subadult, Adult. Adult body proportions are achieved at around 40 mm DML (the Juvenile 2 stage), and onset of sexual maturity occurs at 150 mm DML. The squid used in our experiments include four of Segawa's life history stages: Hatchling (up to 10 mm DML), Juvenile 1 (11–25 mm DML), Juvenile 2 (26–40 mm DML) and Young 2 (60–100 mm DML). We did not use squid from life history stages later than Juvenile 2 for the analysis of muscle ultrastructure because previous studies of *S. lessoniana* demonstrated that ontogenetic changes in the kinematics of the mantle and the gross organization of the muscles and connective tissues of the mantle are complete before the onset of the Juvenile 2 stage (Thompson and Kier, 2001a,b).

The squid, all of which were in excellent condition, were maintained in circular aquaria and used in a series of experiments to measure ontogenetic changes in the

mechanics and kinematics of the mantle (see Thompson and Kier, 2001b, 2002) and the kinematics of the escape jet (J. T. Thompson and K. M. Lobo, in preparation). Care and maintenance of the squid followed the animal care guidelines of the University of North Carolina at Chapel Hill and St Joseph's University.

Transmission electron microscopy

Five hatchlings and four juveniles were over-anesthetized in $MgCl_2$ (Messenger et al., 1985) and killed by decapitation. All of the juveniles were from the Juvenile 2 stage (Segawa, 1987). Portions of mantle tissue were excised from the ventral midline near ½ dorsal mantle length and fixed at 4°C in 3.0% glutaraldehyde, 0.065 mol l^{-1} phosphate buffer, 0.5% tannic acid and 6% sucrose for 8–12 h (Kier, 1996). After fixation, the tissue was transferred to chilled 0.065 mol l^{-1} phosphate buffer, 1% glutaraldehyde, 6% sucrose and stored at 4°C until the entire ontogenetic series was fixed. The tissue was then postfixed for 40 min at 4°C in a 1:1 solution of 2% osmium tetroxide and 2% potassium ferrocyanide in 0.13 mol l^{-1} cacodylate buffer (Kier, 1996). The tissue was rinsed in chilled 0.13 mol l^{-1} cacodylate buffer for 15 min, dehydrated in a graded series of acetones and embedded in epoxy resin (Epox 812; Ernest F. Fullam, Latham, NY, USA).

The processes of fixation, dehydration and embedding may cause shrinkage of cells and connective tissues. Page and Huxley (1963) found that A-band lengths of various frog striated skeletal muscles suffered minimal shrinkage relative to other methods when fixed in buffered glutaraldehyde and dehydrated in acetone. Thus, we adopted their protocol in an attempt to minimize the effects of tissue processing on measurements of myofilament lengths.

Embedded tissue blocks were sectioned in planes perpendicular to the longitudinal axis of the mantle (i.e. parallel to the long axes of the circular muscles) using a diamond knife. Thick sections (0.5–1 μm) were cut initially and stained in an aqueous solution of 0.1% Toluidine Blue and 0.1% sodium borate. Sections were then examined using bright-field microscopy to help align the long axes of the circular muscle fibres parallel to the knife edge. Once alignment was achieved, thin sections (gold to silver interference colour) were cut, mounted on grids and stained with saturated aqueous uranyl acetate and Reynolds lead citrate (Reynolds, 1963). Thin sections were examined with either a Zeiss EM-10CA or JEOL JEM 1010 transmission electron microscope, and portions of the sections that met our criteria (see Morphometrics) were photographed.

Light microscopy

Ontogenetic changes in the ratio of SMR to CMP fibres were investigated as follows. Small blocks of tissue were excised from the ventral midline of the mantle near ½ dorsal mantle length, fixed for 72 h in buffered formalin, dehydrated in a graded series of ethanol up to 95%, and then embedded in glycol methacrylate plastic (JB-4; Polysciences, Inc., Warrington, PA, USA). The tissue blocks were sectioned at 1.0–2.0 μm in a plane perpendicular to the long axes of the circular muscle fibres and stained in solutions of either 0.1% Toluidine Blue and sodium borate or Basic Fuchsin–Toluidine Blue (Bourne and St John, 1978). The stained slides were examined using bright-field microscopy.

Morphometrics

Thick filament lengths were measured on the electron micrographs using calipers. Because the circular muscle fibres of squid are fusiform in shape (Bone et al., 1995) and obliquely striated (Hanson and Lowy, 1957; Lowy and Hanson, 1962; Millman, 1967), it is often difficult to confirm that the section plane is parallel to the longitudinal axis of the fibre and thus to ensure that an individual thick filament remains in the section plane along its entire length. As described above, an attempt was made to carefully align the section plane during ultramicrotomy, and care was taken to measure thick filaments only from fibres (1) in which the diameter of the mitochondrial core remained constant over the length of the fibre (suggesting that the long axis of the fibre was parallel to the section plane) and (2) that spanned at least two electron microscope grid bars. Because of the difficulties associated with section plane alignment, however, the thick filament lengths we report here may be underestimates.

We measured thick filaments from a minimum of two SMR and two CMP circular muscle fibres per animal. A minimum of 200 thick filaments was measured in each animal.

In a minimum of 10 muscle fibres from each animal, we also measured (1) the maximum diameters of SMR and CMP circular muscle fibres and (2) the diameter of the mitochondrial core in each fibre from the transmission electron micrographs of longitudinal sections of the fibres. From these data, we explored ontogenetic changes in muscle fibre size and the cross-sectional area of the muscle fibre occupied by myofilaments. Note that a given longitudinal section will not pass through the middle of all fibres in the section, and thus our measurements do not estimate the actual maximum diameter of the fibres. Because the sections sample fibres at a variety of locations randomly, however, differences in the mean diameter measured for one sample *versus* another reflect actual differences in the size distribution of the cells. It might be argued that transverse sections would avoid this difficulty, and while this would be true for cylindrical objects, the fusiform shape of the fibres means that a given section will also not necessarily pass through the widest portion of the cell. Thus, our approach reveals relative differences in the size distribution of the cells but will not necessarily provide an absolute estimate of the average maximum diameter or area.

Finally, we estimated the ratio of SMR and CMP muscle fibres from the sections of tissue blocks embedded in glycol methacrylate. On each tissue section, all of the circular muscle cells in a portion of the mantle that included the entire thickness of the mantle wall were counted and scored as either SMR or CMP.

Mantle kinematics

We used two methods to measure mantle kinematics during the escape jet. The first is described and critiqued in detail elsewhere (see Thompson and Kier, 2001a) and we include a brief description here. We attempted initially to measure the kinematics of the mantle during escape-jet locomotion in free-swimming squid. The small size of the hatchlings made it difficult to videotape at high magnification and thus to obtain adequate spatial resolution for the kinematics measurements. To allow videotaping at high magnification and to increase the spatial resolution of the edges of the mantle, and hence the accuracy of the kinematics measurements, the squid were tethered in the field of view of the camera.

Individual squid were anesthetized lightly in a 1:1 solution of 7.5% $MgCl_2$:artificial seawater (Messenger et al., 1985). Following anaesthesia, the squid were tethered. A needle (0.3 mm-diameter insect pin for smaller animals or 0.7 mm-diameter hypodermic needle for larger animals) was inserted through the brachial web of the squid, anterior to the brain cartilage and posterior to the buccal mass. The needle was positioned between these two rigid structures to prevent it from tearing the soft tissue of the squid. The needle was inserted into a hollow stainless steel post (hypodermic tubing) attached to a sheet of acrylic plastic. The needle fitted tightly in the hollow post to prevent movement. Flat, polyethylene washers on the post and needle were positioned above and below the head to prevent vertical movement.

Insertion of the needle through the anesthetized squid was rapid and required minimal handling of the animal. *S. lessoniana* become nearly transparent under anaesthesia, making the buccal mass and the brain cartilage readily visible. Needle placement was verified after the experiment by examination of the location of the needle entrance and exit wounds.

Tethered squid were transferred to the bottom of the video arena (0.4 m long × 0.2 m wide × 0.15 m deep), which was filled with aerated 23°C artificial seawater, and allowed to recover. The squid were at least five body diameters away from both the surface of the water and the bottom of the tank to reduce the possibility of surface interactions affecting mantle kinematics.

Although tethering is an invasive technique, there were several indications that it was not unduly traumatic to the squid. First, tethered squid behaved similarly to the animals in the holding tank. Both the tethered and free-swimming squid spent most of the time hovering using the fins and low-amplitude jets. Second, unlike squid that are in distress or startled, the majority (>90%) of the tethered animals did not eject ink. Third, the chromatophore patterns of tethered squid did not differ qualitatively from the patterns exhibited by the free-swimming squid in the holding tank. Finally, squid that were untethered and returned to the holding tank swam normally and could survive for several hours. It is not known how long these animals could have survived because all the animals were killed for histological analysis after the day's experiments were completed.

Escape jet behaviour was elicited by tapping on the glass of the recording arena and was recorded from above with a Panasonic AG-450 S-VHS professional video camera recorder. The camera was adjusted so that the squid filled as much of the field of view as possible. To maximize the measurement resolution, the animal was oriented with the long axis of the mantle vertical in the video field (i.e. perpendicular to the video scan lines). The animals were free to rotate around the tether during the experiments but most remained in the original orientation. The frame rate of the camera (60 video fields per second) was more than 10 times faster than the observed frequency of the mantle jetting cycle. To reduce image blur, the high-speed shutter of the camera was set at 1/1000 s. Illumination was adjusted *via* a variac to the minimum level necessary to provide good contrast between the squid and the background.

Videotapes were analyzed using a Panasonic AG-1980P professional S-VHS video cassette recorder to identify escape-jet sequences suitable for digitizing. Only those sequences in which the mantle remained in the same orientation (i.e. the mantle remained nearly horizontal and did not twist relative to the head) were digitized. Individual video fields were digitized using an Imagenation (Beaverton, OR, USA) PXC200 frame grabber card.

Mantle diameter changes during vigorous escape jets were measured from digitized video fields using morphometrics software (SigmaScan Pro 4.0; SPSS Science, Chicago, IL, USA). Diameter at ⅓ of the DML (from dorsal mantle edge) was measured in each video field prior to the start of and throughout the duration of an escape jet. The mantle diameter at ⅓ DML was selected because the greatest-amplitude mantle movements occurred at this location in all squid examined. We normalized the data by dividing the mantle diameter measured in each video field by the resting mantle diameter (= mantle diameter of the anesthetized animal at ⅓ DML) of the squid. Normalization by the resting mantle diameter standardized the analysis of mantle contraction data among the squid and allowed for comparisons between animals of different size. Numerous escape-jet sequences were analyzed from each animal. Only the sequences with the largest mantle contraction were reported.

The mantle diameter data were plotted against time. Time was estimated from the video camera frame rate (approximately 0.017 s per video field). The rate of mantle contraction was determined by dividing the mantle diameter change between successive video fields by 0.017 s. This calculation yielded a set of incremental rates of mantle contraction. The highest incremental rate was reported as the maximum mantle contraction rate for that animal.

The second method used two high-speed digital video cameras (Photron 10K-PCI; Photron, Inc., San Diego, CA, USA) to record escape-jet behaviour in freely swimming squids. The cameras were positioned with their optical axes at 90° to one another, and escape jets were recorded at 250 frames s^{-1}. Of the numerous escape jets recorded, three permitted accurate measurement of mantle kinematics. In these

sequences, the squid remained in one plane throughout the jet, with the dorsal midline of the mantle facing one camera, allowing the edges of the mantle to be resolved clearly. We measured the maximum rate of mantle diameter change from one camera following a similar procedure to that outlined above with the exception that Photron Motion Tools (Photron, Inc.) software was used to track the change in mantle diameter with time.

Harper and Blake (1989) have shown that although digitizing film or video of animal movements can provide accurate position–time data, velocities and accelerations calculated from such data may be overly smoothed. This inherent error decreases with increasing camera frame rate. Because most of the kinematics data were collected at a relatively low sampling rate (60 Hz), the maximum mantle contraction rates we report are likely to be underestimates. Furthermore, this error is likely to be greater for hatchlings than for juveniles because the duration of mantle contraction is shorter in the hatchlings and thus there are fewer position–time data points for each hatchling jet cycle. Thus, the maximum mantle contraction rates for hatchlings are probably underestimated to a greater extent than those of the larger squids.

Statistics

The mantle kinematics data from each stage were compared with a one-way analysis of variance (ANOVA). Pair-wise comparisons were made using the Student–Newman–Keuls method of comparison (Zar, 1996). This analysis was appropriate because the data in each stage were distributed normally (Kolmogorov–Smirnov goodness of fit test, $P>0.4$ for each stage; Zar, 1996).

Comparisons of thick filament length between animals and within one individual were made with a one-way ANOVA. Pair-wise comparisons were made using the Student–Newman–Keuls method of comparison (Zar, 1996). All statistical comparisons were made using SPSS for Windows 12.0 (SPSS, Inc., Chicago, IL, USA).

Table 1. *Ontogeny of thick myofilament length*

Life history stage	SMR fibres (μm)	CMP fibres (μm)
Hatchling (*N*=5, *n*=1063)	1.0±0.05 (0.7–1.4)	1.0±0.04 (0.7–1.4)
Juvenile 2 (*N*=4, *n*=1127)	1.9±0.8 (1.2–3.4)	1.5±0.1 (0.9–2.2)

Ontogeny of thick myofilament length of the circular muscles of the mantle, measured from transmission electron micrographs. Values are means ± s.d. Numbers in parentheses indicate the range of measurements. One-way ANOVA (Student–Newman–Keuls comparison) results are as follows: Hatch SMR *vs* Hatch CMP, $P=0.84$; Hatch CMP *vs* Juvenile 2 CMP, $P<0.001$; Hatch SMR *vs* Juvenile 2 SMR, $P<0.001$; Juvenile 2 SMR *vs* Juvenile 2 CMP, $P<0.01$. CMP, central mitochondria-poor circular muscle fibres; SMR, superficial mitochondria-rich circular muscle fibres; *N*, number of animals; *n*, number of thick filaments measured.

Results

Ontogeny of thick filament lengths

The thick filament lengths of both the SMR and CMP circular muscles of the mantle increased significantly during the ontogeny of oval squid *Sepioteuthis lessoniana* (Table 1; Figs 4, 5).

Within an individual hatchling, there was no significant difference between the thick filament lengths of the SMR and the CMP circular muscle fibres. Within an individual juvenile, however, the thick filaments of the SMR fibres were

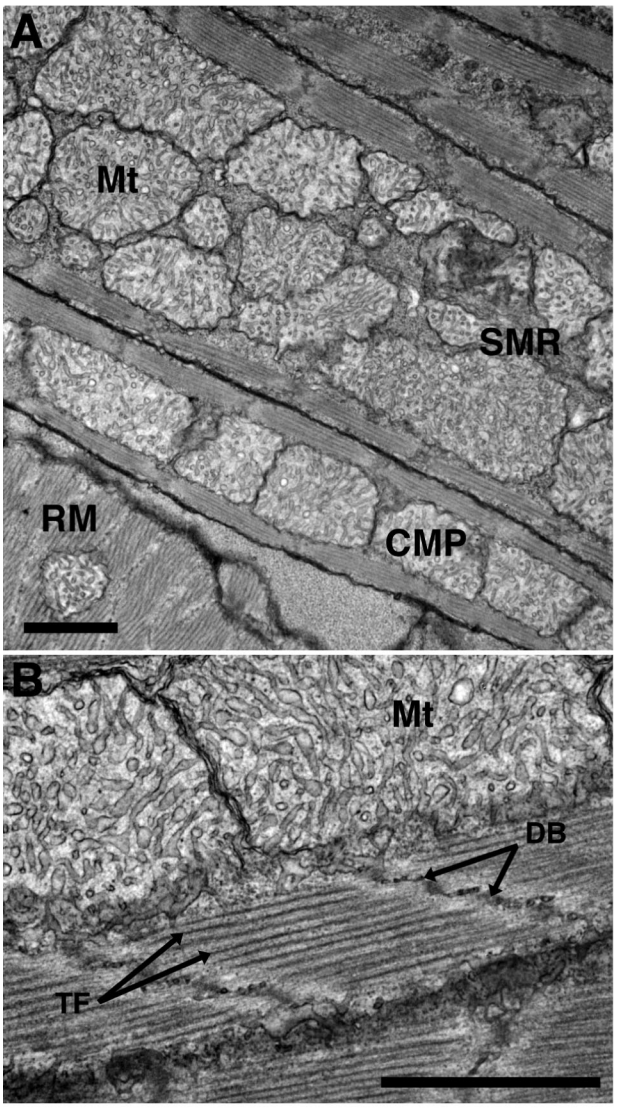

Fig. 4. Transmission electron micrographs of transverse sections of the ventral mantle of a newly hatched *Sepioteuthis lessoniana* showing circular muscle fibres cut parallel to their long axes. (A) View of a superficial mitochondria-rich (SMR) and a central mitochondria-poor (CMP) circular muscle fibre. Note the core of mitochondria (Mt) in each. A radial muscle cell (RM) is also visible. (B) Magnified view of a CMP muscle cell showing a single sarcomere and its thick filaments (TF). Note that the length of the thick filaments is about 1 μm. The scale bar in each panel is 1 μm. DB, dense bodies.

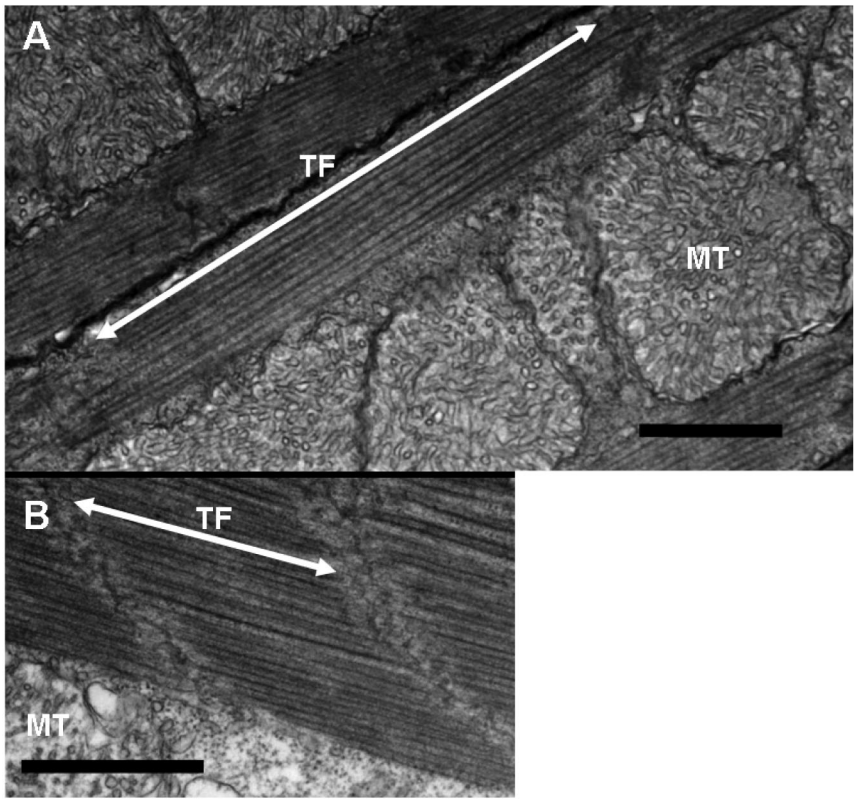

Fig. 5. Transmission electron micrographs of transverse sections of the ventral mantle of a juvenile *Sepioteuthis lessoniana* showing circular muscle fibres cut parallel to their long axes. (A) Portion of a superficial mitochondria-rich (SMR) muscle fibre to illustrate the length of the thick filaments (TF). The approximate dimensions of the sarcomere and the long axis of the thick filaments are indicated by the arrow. Note that the lengths of the longest thick filaments are 4–5 μm. (B) View of a central mitochondria-poor (CMP) cell that shows a portion of one sarcomere. The arrow indicates the approximate length of one sarcomere and the long axis of the thick filaments. Note that the lengths of the longest thick filaments are ~1.5 μm. Scale bars, 1 μm. MT, mitochondria.

approximately 25% longer than those in the CMP fibres (Table 1).

Ontogeny of SMR and CMP dimensions

The mean estimated diameter of the SMR and CMP circular muscle fibres increased significantly during ontogeny while the mitochondrial cores of the SMR and CMP fibres increased in mean estimated diameter relatively little (Table 2; Figs 2, 3). Within an individual juvenile or hatchling squid, the mean estimated cross-sectional area of the muscle fibre occupied by myofilaments did not differ significantly between SMR and CMP muscle fibres. During ontogeny, however, the mean estimated cross-sectional area of the fibre occupied by myofilaments increased significantly for both CMP and SMR circular muscle fibres. In the CMP muscle fibres, myofilaments composed 8.8±0.94 μm^2 of the cross-sectional area of the fibre in juveniles and only 3.7±0.25 μm^2 in hatchlings; these values correspond to 89% and 75%, respectively, of the cross-sectional area of the muscle fibre. In the SMR muscle fibres, myofilaments composed 8.6±0.26 μm^2 in juveniles and 4.2±0.26 μm^2 in hatchlings. These values correspond to 56% and 45% of the cross-sectional area of the fibre in juveniles and hatchlings, respectively (Table 2).

Ontogeny of the relative abundance of SMR and CMP fibres

The relative abundance of CMP circular muscle fibres

Table 2. *Ontogeny of muscle fibre dimensions*

	SMR fibres			CMP fibres		
Life history stage	Fibre diameter (μm)	Core diameter (μm)	Myofilament area (μm^2)	Fibre diameter (μm)	Core diameter (μm)	Myofilament area (μm^2)
Hatchling (*N*=5, *n*=10)	3.5±0.63	2.6±0.63	4.2±0.26 (45%)	2.7±0.30	1.2±0.30	3.7±0.25 (75%)
Juvenile 2 (*N*=4, *n*=10)	4.4±0.42	2.9±0.37	8.6±.26 (56%)	3.6±0.89	1.2±0.36	8.8±0.94 (89%)

Ontogeny of the estimated fibre diameter, mitochondrial core diameter and myofilament area of the circular muscles of the mantle, measured from transmission electron micrographs. Values are means ± s.d.; the percent of the total cross-sectional area of the fibre occupied by myofilaments is listed in parentheses. Within a life history stage, SMR fibre diameter was significantly different from CMP fibre diameter ($P<0.05$), SMR core diameter was significantly different from CMP core diameter ($P<0.005$), and SMR myofilament area was significantly different from CMP myofilament area ($P\ll0.001$; one-way ANOVA, Student–Newman–Keuls comparison). With the exception of CMP core diameter, all comparisons between life history stages were significantly different ($P<0.05$; one-way ANOVA, Student–Newman–Keuls comparison). CMP, central mitochondria-poor circular muscle fibres; SMR, superficial mitochondria-rich circular muscle fibres; *N*, number of animals; *n*, number of CMP and SMR cells measured per animal.

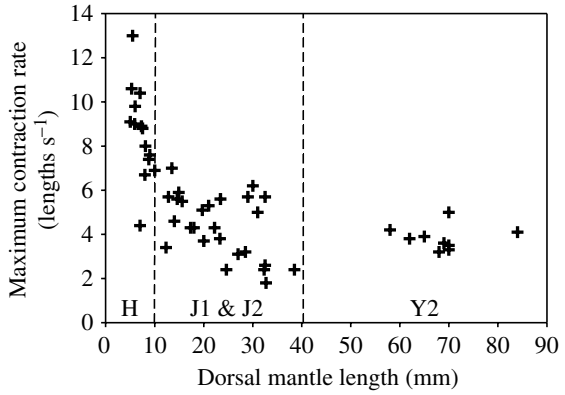

Fig. 6. Plot showing an ontogenetic change in the maximum rate of mantle contraction. Each point represents the maximum rate of mantle contraction during the escape jet for one individual. H, J1, J2 and Y2 refer to the life history stages of Segawa (1987) and correspond to Hatchling, Juvenile 1, Juvenile 2 and Young 2, respectively. See Materials and methods for more detail on the life history stages of Segawa.

increased during growth. The ratio of CMP to SMR fibres increased from approximately 6:1 in hatchlings to approximately 23:1 in the Juvenile 2 stage animals (Figs 2, 3).

Mantle kinematics

The maximum rate of mantle contraction during the escape jet was highest in newly hatched squid and declined during ontogeny (Fig. 6). The maximum rate of mantle contraction at 23°C varied from seven to 13 muscle lengths per second in newly hatched squid and from three to five muscle lengths per second in the Juvenile 1, Juvenile 2 and Young 2 stage animals (Table 3; Fig. 6). A one-way ANOVA among the life history stages (Segawa, 1987) indicated that Hatchling stage *S. lessoniana* had a significantly greater maximum rate of mantle contraction during the escape jet than all other life history stages (Student–Newman–Keuls comparison, $P<0.05$; Table 3).

Table 3. *Mantle contraction rate during the escape jet*

Life history stage	Maximum contraction rate (lengths s^{-1})
Hatchling	8.6±2.1 (14)
Juvenile 1	4.8±1.2 (16)
Juvenile 2	3.8±1.7 (10)
Young 2	3.8±0.55 (9)

The mean maximum mantle contraction rates during the escape jet are listed ± the s.d. of the mean. The number of squid in the sample is in parentheses. The maximum mantle contraction rate for all squid in a life history stage was pooled to calculate the mean and the s.d. The mean value for the Hatchling stage squid was significantly different from the mean for the Juvenile 1, Juvenile 2 and Young 2 life history stages (one-way ANOVA, Student–Newman–Keuls comparison, $P<0.05$). Other within-column comparisons of mantle contraction rate were not significantly different.

Discussion

The dimensions of the myofilaments have a significant effect not only on the mechanical properties of the circular muscles of the mantle, but may also affect the kinematics and mechanics of jet locomotion. It is surprising, therefore, that although the ultrastructure of the circular mantle muscles of squids has been documented previously (Millman, 1967; Ward and Wainwright, 1972; Moon and Hulbert, 1975; Bone et al., 1981; Preuss et al., 1997), there is only one estimate of thick filament length. Millman (1967) reported a thick filament length of 1.5 μm in the circular mantle muscles of *Loligo* spp. He did not indicate the age or size of the animal or from where in the mantle he sampled (which is understandable because the distinction between SMR and CMP fibres was not recognized until 1981; see Bone et al., 1981; Mommsen et al., 1981). The length reported by Millman (1967) is within the range of both the SMR and CMP circular muscles of juvenile *S. lessoniana* reported here.

Ontogenetic changes in the mechanical properties, metabolism and neural activation of striated muscles are common. It is unclear if such changes represent developmental constraints, selection for different levels of performance during growth, or both. Regardless of the ultimate causes, it is apparent that such changes involve different mechanisms in cephalopods compared with other animals. In the vertebrates, the ontogeny of the contractile properties of muscle involves differential expression of isoforms of myosin (e.g. Goldspink, 1983; Gondret et al., 1996) but no change in myofilament dimensions. The extensor digitorum longus of newborn rabbits, for example, is physiologically slow-contracting, but contraction velocity increases rapidly in the first few weeks after birth (Gauthier et al., 1978). The increase in contraction velocity is accompanied by a change in the amount of the fast-twitch myosin ATPase that is synthesized in the muscle (Gauthier et al., 1978). Although sarcomere lengths increase slightly during the growth of rabbits, there is no change in the lengths of either the thick or thin filaments (Goldspink, 1968; Gauthier et al., 1978).

Unlike the vertebrates, the mechanical properties of cephalopod striated muscles appear to be modulated structurally rather than biochemically. For example, the arms and tentacles of many species of squids are similar in their gross anatomy and muscular arrangement, yet the tentacles are elongated with remarkable rapidity during prey capture while the arms are inextensible and perform slower bending and twisting movements (Kier, 1982). Comparison of the protein profiles of myofilaments from the transverse muscle of the arms and tentacles (the muscle responsible for elongation in the tentacles and bending support in the arms) using a variety of sodium dodecyl sulphate polyacrylamide gel electrophoresis (SDS-PAGE) techniques, along with cyanogen bromide and V8 protease peptide mapping of the myosin heavy chains, showed little evidence of differences in contractile protein isoforms (Kier, 1991; Kier and Schachat, 1992). There are, however, substantial differences in the ultrastructure of the muscles of the arms and tentacles (Kier, 1985). The transverse

muscles of the tentacles are composed of cross-striated fibres while the serially homologous transverse muscle in the arms consists of obliquely striated fibres (Kier, 1985). The thick filaments of the cross-striated transverse muscles of the tentacles are unusually short, ranging from approximately 0.5 to 1.0 μm (Kier, 1985; Kier and Curtin, 2002). The short thick filaments of the tentacles result in a greater number of sarcomeres in series per unit length and, since shortening velocities of elements in series are additive, confer high shortening velocity (15.4 lengths s^{-1}) on the transverse muscle mass, thereby permitting the rapid elongation of the tentacles during the prey strike (Kier and Curtin, 2002; see Josephson, 1975). By contrast, the thick filaments of the obliquely striated muscle mass of the arms range from approximately 6 to 7.5 μm (Kier, 1985; Kier and Curtin, 2002), resulting in much lower shortening velocity (1.5 lengths s^{-1}) (Kier and Curtin, 2002).

In the vertebrates, myofilament dimensions remain constant throughout growth (Goldspink, 1968, 1983). If the relatively short thick filaments of hatchling *S. lessoniana* represent selection for higher shortening velocity, it highlights what may be a fundamental difference in the modulation of muscle mechanical properties between cephalopods and vertebrates.

The ontogenetic increase in thick filament length we report is not unique to the circular muscles of *S. lessoniana*. The thick filaments of the obliquely striated transverse muscles of the arms of *S. lessoniana* also increase in length during ontogeny, from 2.2 μm in hatchlings to 6.4 μm in adults (Kier, 1996). Interestingly, the thick filament lengths of the cross-striated transverse muscles of the tentacles decrease from 2.4 to 1.2 μm during the same interval (Kier, 1996). The ontogenetic change in thick filament length of the tentacle muscle is clearly related to changing function of the tentacles, although the functional basis for the arm muscle change is less clear (Kier, 1996).

Despite the similar trend in the arm transverse muscles, the ontogenetic increase in thick filament length we describe for the circular muscles of *S. lessoniana* squid may be unique among animals with precocious offspring. In adult vertebrates, the sarcomeres of skeletal muscles are approximately 2.4 μm long, with thick filaments from 1.5 to 1.6 μm in length (Hanson and Huxley, 1953; Huxley and Niedergerke, 1954; Huxley, 1957; Huxley and Hanson, 1957). While it is not uncommon for sarcomere lengths to increase slightly during postnatal growth, this does not involve a change in the lengths of either the thick or thin filaments (Goldspink, 1968, 1983). In the flight muscles of *Drosophila melanogaster* and *Anax imperator*, sarcomere length increases from ~1.6 to 3.2 μm during pupation (Valvassori et al., 1978; Reedy and Beall, 1993). Because the thick filaments are nearly the length of the sarcomere, this represents an ontogenetic increase in thick filament length (Valvassori et al., 1978; Reedy and Beall, 1993). This increase occurs, however, during metamorphosis, when the insects are not actively seeking food and avoiding predators. Interestingly, the converse situation occurs in pupating *Manduca sexta*, where the dorsal longitudinal muscle has sarcomeres that are ~1.3 times longer than in the adult (Rheuben and Kammer, 1980).

CMP vs SMR: function during locomotion

The differentiation of the circular muscle into CMP and SMR fibres is hypothesized to be analogous to the subdivisions of red and white muscle observed in the vertebrates (Bone et al., 1981; Mommsen et al., 1981; Rome et al., 1988). The SMR circular muscle fibres, analogous to the red muscles of vertebrates, power the constant ventilatory movements and prolonged slow-speed swimming (Bartol, 2001). The CMP circular muscle fibres, analogous to the white muscles of vertebrates, produce the brief escape jets (Bartol, 2001; Bone et al., 1981; Gosline et al., 1983; Mommsen et al., 1981). These putative roles for the two different types of muscle fibres are supported by EMG recordings in *Lolliguncula brevis* (Bartol, 2001) in which SMR fibres were shown to be active during low-amplitude contractions of the mantle while the CMP fibres were largely quiescent. Conversely, the CMP fibres are active during more rapid swimming (Bartol, 2001).

The difference in thick filament lengths of the SMR and CMP circular muscle fibres of juvenile *S. lessoniana* is consistent with the proposed functional differences. The small cross-sectional area of the SMR fibres relative to the area of the mantle wall (Figs 2, 3) implies a high load during low-amplitude jetting, particularly if the CMP muscles do not contribute substantially to mantle contraction (see Bartol, 2001). Because thick filament length is proportional to the peak isometric tension generated by a striated muscle fibre (Josephson, 1975), the longer thick filaments of the SMR fibres in juvenile *S. lessoniana* may increase the tension produced relative to a hypothetical SMR fibre with thick filaments the same length as in the CMP fibres. In addition, the low-amplitude movements powered by the SMR fibres are slower and thus do not require as high a shortening velocity as occurs during escape jets. By comparison, the CMP muscles appear to be used mainly for vigorous escape jets. Their shorter thick filaments may allow for higher unloaded shortening velocities than in the SMR fibres and more rapid expulsion of water from the mantle cavity, albeit with some decrease in peak tension.

Dimensions of SMR and CMP fibres

It is interesting to note that our estimates of mitochondrial core diameter did not change significantly during the growth of CMP or SMR fibres. Hypertrophy of the fibres appears to occur primarily through addition of myofilaments, not through addition of mitochondria. Within an individual, the absolute area of myofilaments did not, on average, differ between SMR and CMP fibres. This is a surprising finding. In the vertebrates, the total myofilament area of the red and white fibres differs substantially (e.g. Gleeson et al., 1980; Eisenberg, 1983). Thus, SMR fibres seem to differ from CMP fibres only in the dimensions of the core. It is unknown if the isoforms of myosin heavy chain (MHC) differ between the two types of muscle fibres, although two isoforms of MHC that appear to be splicing variants of a single myosin gene have been found in the ventral funnel retractor muscle of the long-finned squid *Loligo pealei* (Matulef et al., 1998).

Ontogeny of jet locomotion

The ontogenetic change in thick filament length we report may have important consequences for the mechanics, kinematics and propulsion efficiency of cephalopod jet locomotion. All coleoid cephalopods (e.g. squids, octopuses, cuttlefishes) can swim using pulsed jets. Squids form a single jet pulse by first expanding the mantle radially so that water fills the mantle cavity through openings at the anterior margin of the mantle (Fig. 1). Once the mantle cavity is full, the circular muscles contract. Contraction increases the pressure in the mantle cavity, closes valves on the intake openings and drives water out of the mantle cavity through the funnel (Fig. 1). Repetition of these movements results in a pulsed jet.

Siekman (1963) and Weihs (1977) predicted that pulsed jetting would increase the total thrust produced relative to a continuous or steady jet because of added mass effects and the entrainment of ambient water into the vortices generated by the pulsed jet. Recent work by Krueger and Gharib (2003) with a mechanical vortex ring generator suggests that at intermediate Reynolds numbers (*Re*), where the effects of viscous and inertial forces are nearly equal, a more highly pulsed jet (i.e. higher frequency of mantle contractions) will generate more thrust than a less-pulsed jet. Moreover, a highly pulsed jet will allow for a lower jet velocity to be used to generate a given thrust, which will ultimately improve propulsive efficiency (Vogel, 1994).

Newly hatched *S. lessoniana* jet in an intermediate Reynolds number fluid regime ($10<Re<100$ during vigorous jetting; K. M. Lobo and J. T. Thompson, unpublished observations; Thompson and Kier, 2001b). The relevance of the work of Krueger and colleagues to the present study is that the shorter thick filaments of newly hatched squids may permit higher shortening velocities for the circular muscles, a greater rate of mantle contraction and thereby allow higher frequency of mantle contractions. This may permit newly hatched squid to generate a more highly pulsed jet than if they had thick filaments the same length as the juvenile squid.

Ontogeny of mantle kinematics

The ontogenetic increase in thick filament length suggests that the contractile properties of the circular muscles change during growth. The shortening velocity of striated muscles, such as the obliquely striated circular muscles of the mantle, depends on the lengths of the thick filaments and sarcomeres, the load of the muscle and the rate of cross-bridge cycling (e.g. Josephson, 1975). Thick filament length is inversely proportional to shortening velocity and directly proportional to peak isometric tension (Millman, 1967; Josephson, 1975). Assuming all else is equal, we predict that the circular muscles of newly hatched *S. lessoniana* will produce lower peak isometric tensions and higher unloaded shortening velocities than the circular muscles of juvenile and adult squid.

The measurements of whole-mantle kinematics during escape-jet locomotion provide partial support for this prediction. The maximum rate of mantle contraction is highest in newly hatched squid and declines during ontogeny. At 23°C, the maximum rate of mantle contraction was 8.6±2.1 circumference lengths s^{-1} in hatchlings but only 3.8±0.55 lengths s^{-1} in juveniles and Young 2 animals. We do not know, however, the loading of the circular muscle fibres during the jet, and there is no information on potential changes in the cross-bridge cycling rate during ontogeny. Thus, a definitive test of the predicted change in muscle fibre properties awaits direct measurements of the contractile mechanics of the circular muscles during ontogeny.

In summary, the lengths of the thick filaments of the circular muscles of the mantle of oval squid increase significantly during ontogeny. The change in thick filament length may alter the contractile properties of the circular muscles and may also underlie the significant decrease in the rate of mantle contraction that occurs during ontogeny. Ontogenetic changes in thick filament length may highlight a fundamental difference in the modulation of muscle mechanical properties between cephalopods and vertebrates.

We thank S. Guarda for able assistance with ultramicrotomy, staining, printing of negatives and morphometrics. We also thank T. Perdue and L. Crescenti for help with the electron microscopy. We thank J. Forsythe and L. Walsh of the National Resource Center for Cephalopods (NRCC), University of Texas Medical Branch, Galveston, TX, USA for assistance in providing specimens. The research was supported by the following sources: (1) a Seeding Postdoctoral Innovators in Research and Education (SPIRE) fellowship to J.T.T. from the Minority Opportunities in Research Division of the National Institute of General Medical Sciences (Grant No. GM000678), (2) NSF grant IOB-0446081 (to Ian Bartol, J.T.T. and Paul Krueger), and (3) NSF grant IBN-972707 to W.M.K.

References

Bartol, I. K. (2001). Role of aerobic and anaerobic circular mantle muscle fibers in swimming squid: electromyography. *Biol. Bull.* **200**, 59-66.

Boletzky, S. v. (1974). The "larvae" of Cephalopoda: a review. *Thalassia Jugoslavica* **10**, 45-76.

Bone, Q., Pulsford, A. and Chubb, A. D. (1981). Squid mantle muscle. *J. Mar. Biol. Assoc. UK* **61**, 327-342.

Bone, Q., Brown, E. R. and Usher, M. (1995). The structure and physiology of cephalopod muscle fibres. In *Cephalopod Neurobiology* (ed. N. J. Abbott, R. Williamson and L. Maddock), pp. 301-329. New York: Oxford University Press.

Bourne, C. A. J. and St. John, D. J. (1978). Improved procedure for polychromatic staining of epoxy sections with basic fuchsin–toluidine blue. *Med. Lab. Sci.* **35**, 399-400.

Buller, A. J., Eccles, J. C. and Eccles, R. M. (1960). Differentiation of fast and slow muscles in the cat hindlimb. *J. Physiol.* **150**, 399-416.

Calder, W. A. (1984). *Size, Function, and Life History*. Cambridge: Harvard University Press.

Chen, D. S., Dykhuizen, G. v., Hodge, J. and Gilly, W. F. (1996). Ontogeny of copepod predation in juvenile squid (*Loligo opalescens*). *Biol. Bull.* **190**, 69-81.

Eisenberg, B. R. (1983). Quantitative ultrastructure of mammalian skeletal muscle. In *Handbook of Physiology. Section **10**, Skeletal Muscle* (ed. L. D. Peachey), pp. 73-112. Bethesda, MD: American Physiological Society.

Fitzhugh, G. H. and Marden, J. H. (1997). Maturational changes in troponin T expression, calcium sensitivity, and twitch contraction kinetics in dragonfly flight muscle. *J. Exp. Biol.* **200**, 1473-1482.

Gauthier, G. F., Lowey, S. and Hobbs, A. (1978). Fast and slow myosin in developing muscle fibres. *Nature* **274**, 27-29.
Gleeson, T. T., Putnam, R. W. and Bennett, A. F. (1980). Histochemical, enzymatic, and contractile properties of skeletal muscle fibers in the lizard *Dipsosaurus dorsalis*. *J. Exp. Zool.* **214**, 293-302.
Goldspink, G. (1968). Sarcomere length during the post-natal growth of mammalian muscle fibres. *J. Cell Sci*. **3**, 539-548.
Goldspink, G. (1983). Alterations in myofibril size and structure during growth, exercise, and changes in environmental temperature. In *Handbook of Physiology. Section **10**, Skeletal Muscle* (ed. L. D. Peachey), pp. 539-554. Bethesda, MD: American Physiological Society.
Gondret, F., Lefaucheur, L., D'Albis, A. and Bonneau, M. (1996). Myosin isoform transitions in four rabbit muscles during postnatal growth. *J. Muscle Res. Cell Motil*. **17**, 657-667.
Gosline, J. M., Steeves, J. D., Harman, A. D. and DeMont, M. E. (1983). Patterns of circular and radial mantle muscle activity in respiration and jetting of the squid *Loligo opalescens*. *J. Exp. Biol.* **104**, 97-109.
Hanlon, R. T., Forsythe, J. W. and Boletzky, S. v. (1985). Field and laboratory behavior of "Macrotritopus larvae" reared to *Octopus defilippi* Verany, 1851 (Mollusca: Cephalopoda). *Vie Milieu* **35**, 237-242.
Hanson, J. and Huxley, H. E. (1953). Structural basis of the cross-striations in muscle. *Nature* **172**, 530-532.
Hanson, J. and Lowy, J. (1957). Structure of smooth muscles. *Nature* **180**, 906-909.
Harper, D. G. and Blake, R. W. (1989). A critical analysis of the use of high-speed film to determine the maximum accelerations of fish. *J. Exp. Biol*. **142**, 465-471.
Huxley, A. F. and Niedergerke, R. (1954). Structural changes in muscle during contraction. Interference microscopy of living muscle fibres. *Nature* **173**, 971-973.
Huxley, H. E. (1957). The double array of filaments in cross-striated muscle. *J. Biophys. Biochem. Cytol*. **3**, 631-648.
Huxley, H. E. and Hanson, J. (1957). Quantitative studies on the structure of cross-striated myofibrils. 1. Investigations by interference microscopy. *Biochim. Biophys. Acta* **23**, 229-249.
Josephson, R. K. (1975). Extensive and intensive factors determining the performance of striated muscle. *J. Exp. Zool.* **194**, 135-154.
Kawaguti, S. and Ikemoto, N. (1957). Electron microscopy of the smooth muscle of a cuttlefish, *Sepia esculenta* Hoyle. *Biol. J. Okayama Univ*. **3**, 196-208.
Kelly, A. M. (1983). Emergence of specialization in skeletal muscle. In *Handbook of Physiology. Section **10**, Skeletal Muscle* (ed. L. D. Peachey), pp. 507-537. Bethesda, MD: American Physiological Society.
Kier, W. M. (1982). The functional morphology of the musculature of squid (Loliginidae) arms and tentacles. *J. Morphol.* **172**, 179-192.
Kier, W. M. (1985). The musculature of squid arms and tentacles: ultrastructural evidence for functional differences. *J. Morphol.* **185**, 223-239.
Kier, W. M. (1991). Squid cross-striated muscle: the evolution of a specialized muscle fiber type. *Bull. Mar. Sci.* **49**, 389-403.
Kier, W. M. (1996). Muscle development in squid: ultrastructural differentiation of a specialized muscle fiber type. *J. Morphol.* **229**, 271-288.
Kier, W. M. and Schachat, F. H. (1992). Biochemical comparison of fast- and slow-contracting squid muscle. *J. Exp. Biol.* **168**, 41-56.
Kier, W. M. and Curtin, N. A. (2002). Fast muscle in squid (*Loligo pealei*): contractile properties of a specialized muscle fibre type. *J. Exp. Biol.* **205**, 1907-1916.
Krueger, P. S. and Gharib, M. (2003). The significance of vortex ring formation to the impulse and thrust of a starting jet. *Phys. Fluid* **15**, 1271-1281.
Lee, P. G., Turk, P. E., Yang, W. T. and Hanlon, R. T. (1994). Biological characteristics and biomedical applications of the squid *Sepioteuthis lessoniana* cultured through multiple generations. *Biol. Bull.* **186**, 328-341.
Lowy, J. and Hanson, J. (1962). Ultrastructure of invertebrate smooth muscles. *Physiol. Rev*. **42**, S34-S47.
Marceau, F. (1905). Recherches sur la structure des muscles du manteau des Céphalopodes en rapport avec leur mode du contraction. *Trav. Lab. Soc. Sci. Arachon. Ann.* **8**, 48-63.
Marden, J. H., Fitzhugh, G. H. and Wolf, M. R. (1998). From molecules to mating success: integrative biology of muscle maturation in a dragonfly. *Am. Zool.* **38**, 528-544.
Marliave, J. B. (1980). Neustonic feeding in early larvae of *Octopus dofleini* (Wülker). *Veliger* **23**, 350-351.
Matulef, K., Sirokmán, K., Perreault-Micale, C. L. and Szent-Györgyi, A. G. (1998). Amino-acid sequence of squid myosin heavy chain. *J. Muscle Res. Cell Motil*. **19**, 705-712.
Messenger, J. B., Nixon, M. and Ryan, K. P. (1985). Magnesium chloride as an anaesthetic for cephalopods. *Comp. Biochem. Physiol.* **82C**, 203-205.
Milligan, B. J., Curtin, N. A. and Bone, Q. (1997). Contractile properties of obliquely striated muscle from the mantle of squid (*Alloteuthis subulata*) and cuttlefish (*Sepia officinalis*). *J. Exp. Biol.* **200**, 2425-2436.
Millman, B. M. (1967). Mechanism of contraction in Molluscan muscle. *Am. Zool.* **7**, 583-591.
Mommsen, T. P., Ballantyne, J., MacDonald, D., Gosline, J. and Hochachka, P. W. (1981). Analogues of red and white muscle in squid mantle. *Proc. Natl. Acad. Sci. USA* **78**, 3274-3278.
Moon, T. W. and Hulbert, W. C. (1975). The ultrastructure of the mantle musculature of the squid *Symplectoteuthis oualaniensis. Comp. Biochem. Physiol.* **52B**, 145-149.
O'Dor, R. K., Helm, P. and Balch, N. (1985). Can rhyncoteuthions suspension feed? (Mollusca: Cephalopoda). *Vie Milieu* **35**, 267-271.
Page, S. G. and Huxley, H. E. (1963). Filament lengths in striated muscle. *J. Cell Biol.* **19**, 369-390.
Preuss, T., Lebaric, Z. N. and Gilly, W. F. (1997). Post-hatching development of circular mantle muscles in the squid *Loligo opalescens*. *Biol. Bull.* **192**, 375-387.
Reedy, M. C. and Beall, C. (1993). Ultrastructure of developing flight muscle in *Drosophila*. I. Assembly of myofibrils. *Dev. Biol.* **160**, 443-465.
Reynolds, E. S. (1963). The use of lead citrate at high pH as an electron-opaque stain in electron microscopy. *J. Cell Biol.* **17**, 208-212.
Rheuben, M. B. and Kammer, A. E. (1980). Comparison of slow larval and fast adult muscle innervated by the same motor neurone. *J. Exp. Biol.* **84**, 103-118.
Rome, L. C., Funke, R. P., Alexander, R. M., Lutz, G., Aldridge, H., Scott, F. and Freadman, M. (1988). Why animals have different muscle fibre types. *Nature* **335**, 824-827.
Segawa, S. (1987). Life history of the oval squid, *Sepioteuthis lessoniana* in Kominato and adjacent waters central Honshu, Japan. *J. Tokyo Univ. Fish*. **74**, 67-105.
Siekman, J. (1963). On a pulsating jet from the end of a tube, with application to the propulsion of certain aquatic animals. *J. Fluid Mech.* **15**, 399-418.
Stearns, S. C. (1992). *The Evolution of Life Histories*. Oxford: Oxford University Press.
Sweeney, M. J., Roper, C. F. E., Mangold, K. M., Clarke, M. R. and Boletzky, S. V. (1992). *Larval and Juvenile Cephalopods: A Manual for their Identification*. Smithsonian Contribution to Zoology, no. 513. Washington, DC: Smithsonian Institute Press.
Thompson, J. T. and Kier, W. M. (2001a). Ontogenetic changes in mantle kinematics during escape-jet locomotion in the oval squid, *Sepioteuthis lessoniana* Lesson, 1830. *Biol. Bull.* **201**, 154-166.
Thompson, J. T. and Kier, W. M. (2001b). Ontogenetic changes in fibrous connective tissue organization in the oval squid, *Sepioteuthis lessoniana* Lesson, 1830. *Biol. Bull.* **201**, 136-153.
Thompson, J. T. and Kier, W. M. (2002). Ontogeny of squid mantle function: changes in the mechanics of escape-jet locomotion in the oval squid, *Sepioteuthis lessoniana* Lesson, 1830. *Biol. Bull.* **203**, 14-26.
Valvassori, R., DeEguileor, M. and Lanzavecchia, G. (1978). Flight muscle differentiation in nymphs of a dragonfly *Anax imperator*. *Tissue Cell* **10**, 167-178.
Villanueva, R., Nozais, C. and Boletzky, S. V. (1995). The planktonic life of octopuses. *Nature* **377**, 107.
Vogel, S. (1994). *Life in Moving Fluids*. 2nd edn. Princeton, NJ: Princeton University Press.
Ward, D. V. and Wainwright, S. A. (1972). Locomotory aspects of squid mantle structure. *J. Zool. Lond.* **167**, 437-449.
Weihs, D. (1977). Periodic jet propulsion of aquatic creatures. *Fortschr. Zool.* **24**, 171-175.
Werner, E. E. (1987). Size, scaling, and the evolution of complex life cycles. In *Size-Structured Populations* (ed. B. Ebenman and L. Persson), pp. 60-81. New York: Springer-Verlag.
Young, J. Z. (1938). The functioning of the giant nerve fibres of the squid. *J. Exp. Biol.* **15**, 170-185.
Zar, J. H. (1996). *Biostatistical Analysis*. Upper Saddle River, NJ: Prentice Hall.